COMBINED NATURAL CONVECTION AND RADIATION IN PRESENCE OF INTERNAL HEAT GENERATION SOURCE IN ABSORBING-EMITTING-SCATTERING MEDIUM

***Nesrine RACHEDI*[a], *Messaoud GUELLAL*[a*] *and Madiha BOUAFIA*[b]**

[a]Laboratoire de Génie des Procédés Chimiques, Université Ferhat Abbas Sétif-1, Sétif 19000, Algeria

[b]Laboratoire de Mécanique et Energétique d'Evry, Université d'Evry, 91020 Evry Cedex, France

[*] Corresponding author; E-mail: mguellal@univ-setif.dz

Numerical investigation of combined laminar natural convection and volumetric radiation with internal heat generation is presented in this paper and computations are performed for a grey gas-filled square cavity whose horizontal walls are adiabatic and vertical walls are differentially heated. The convection is treated under Boussinesq approximation by an approach based on finite-volumes and the volumetric radiation by the discrete ordinates method. Flow and heat transfer characteristics through isotherms, streamlines and average Nusselt numbers have been presented for an external Rayleigh number 10^6*, internal Rayleigh number 0 to* $4\text{x}10^{12}$*, optical thickness 0 to 10 and Albedo 0 to 1. Representative results illustrating the effects of the optical thickness and the internal heat generation on the flow and the temperature distribution within the cavity are presented. The results reveal that the fluid flow and heat transfer are influenced significantly by the volumetric radiation and the internal heat generation. By comparing the solutions in pure convection, the results in combined convection-volumetric radiation show that when the medium is participating, the effect of internal source presence is very important.*

Key words: *Heat generation, Natural convection, volumetric radiation, Numerical simulation, optical thickness, Albedo*

1. Introduction

The phenomenon of natural convection in a two-dimensional cavity is widely encountered in engineering such as solar collectors, cooling of electronic components, solar energy, heat exchangers, nuclear reactors, ovens, etc. Numerical works of these last years have been concentrating more on the study of heat generating components in the electrical and nuclear industries, and flows in rooms due to thermal energy sources[1-4].The recurring configuration is the one of the heated differential cavity constituted by two opposite vertical walls maintained at constant temperatures and two adiabatic horizontal walls.

In recent years, a great number of researches have been focusing on heat transfer study in semi-transparent medium. Among them, we can cite in particular Lauriat [5] who studied natural convection in the presence of volumetric radiation by considering the medium as a gray gas in a two-dimensional vertical cavity with an aspect ratio of between 5 and 20. The P1 approximation of spherical harmonics method has been used for radiative part. The same problem was modeled by Yucel et al.[6] using the discrete ordinates method. In this study, the cavity was a square with four black walls, the Rayleigh number was fixed to $5x10^6$ and the optical thickness was variable. Draoui et al. [7] studied the effect of the Rayleigh number using the method of spherical harmonics P1 in a cavity where the emissivities of the adiabatic walls were zero and the isothermal walls were black. Fusegi and Farouk[8] studied the natural convection coupled to radiation in a differentially heated cavity with all black walls, and filled with a non-grey gas. The radiative model was treated with finite-volumes approach and the radiative quantities were evaluated by the decomposition of spherical harmonics of order 1. Tan and Howel [9] examined the influence of volumetric radiation on natural convection. They proposed the calculation of global radiative and convective fluxes. Colomer et al.[10] treated the coupling of natural convection with volumetric radiation in a differentially heated three-dimensional cavity in transparent and participating media. Ibrahim [11]studied the influence of radiation on natural convection flow in a differentially heated square cavity containing ambient air and used two different configurations with high Rayleigh number. Laouar-Meftah et al.[12] studied the double diffusive natural convection in a square cavity filled with an air-CO_2 mixture with vertical walls maintained at different temperatures and concentrations. Moufekkir et al. [13]and Lari et al.[14]addressed the analysis of the effect of radiative heat transfer on convective heat transfer in a square cavity containing a participating gas under standard ambient conditions. Liu et al. [15]developed a numerical model for simulating natural convection combined to volumetric radiation in absorbing emitting and diffusing medium in a two-dimensional square cavity. Mezrhab et al. [16]presented numerical solutions for the coupling radiation-double diffusive natural convection in a square cavity filled with an absorbing, emitting and non-diffusing grey gas. Byun et al. [17] studied the effects of specularly reflecting wall under the combined radiative and laminar natrural convective heat transfer in an infinite square pipe filled with absorbing and emitting gray medium. Kumar and Eswaran[18] presented a three-dimensional numerical simulation of the coupled thermal radiation and natural convection in a differentially heated rectangular cavity. Chaabane et al. [19]developed a new algorithm for solving natural convection coupled to radiation in a two-dimensional cavity containing an absorbing, emiting and diffusing medium. The radiative transfer equation was solved using control volume finite element method; the density, velocity and temperature fields were calculated using the double population lattice Boltzmann equation. Several other studies have focused on the natural convection combined to surface radiation by analyzing the influence of radiative effects on fluid flows and heat transfer in closed cavities [20-25]. A number of studies have examined the interaction between surface radiation and heat generation in the case of a differentially heated cavity [26-29]. However, the interaction between volumetric radiation and internal heat generation has been little study although volumetric radiation is inherent in natural convection. Thereafter, due to its practical interest, the subject needs further effort to improve the knowledge in this field. In the present work, and following our previous study [30], we propose to extend the analysis performed on the coupling of natural convection with volumetric radiation to include the effect of internal heat generation in a semi-transparent medium contained in a differentially heated cavity. The main objective of the study consists of examining the effect of the internal Rayleigh number, Ra_I, the optical thickness τ and the albedo coefficient ω on fluid flow and heat transfer.

2. Problem formulation

Details of the geometry are shown in fig. 1. It is a square cavity filled with a semi-transparent fluid assumed to be homogeneous, incompressible, laminar, gray and non-scattering, with internal heat generation q. The two vertical walls are black ($\varepsilon_{1,2} = 1$) and maintained at different temperatures T_C and T_H ($T_C < T_H$), while the two horizontal walls are reflective ($\varepsilon_{3,4} = 0$) and perfectly insulated. It will also be assumed that the temperature differences in the flow domain considered are sufficiently small to justify the use of the Boussinesq approximation.

The modeling is based on the Navier–Stokes equations coupled with energy equation and radiative transfer equation (RTE) which provides the term of radiative source to be inserted into the energy equation. The set of these equations is given in dimensional form as:

$$\frac{\partial u}{\partial x} + \frac{\partial v}{\partial y} = 0 \tag{1}$$

$$\rho\left(\frac{\partial u}{\partial t} + u\frac{\partial u}{\partial x} + v\frac{\partial u}{\partial y}\right) = -\frac{\partial P'}{\partial x} + \mu\left(\frac{\partial^2 u}{\partial x^2} + \frac{\partial^2 u}{\partial y^2}\right) \tag{2}$$

$$\rho\left(\frac{\partial v}{\partial t} + u\frac{\partial v}{\partial x} + v\frac{\partial v}{\partial y}\right) = -\frac{\partial P'}{\partial y} + \mu\left(\frac{\partial^2 v}{\partial x^2} + \frac{\partial^2 v}{\partial y^2}\right) + \rho g\beta(T - T_0) \tag{3}$$

$$\rho C_p\left(\frac{\partial T'}{\partial t'} + u\frac{\partial T'}{\partial x} + v\frac{\partial T'}{\partial y}\right) = k\left(\frac{\partial^2 T'}{\partial x^2} + \frac{\partial^2 T'}{\partial y^2}\right) + q - div(\vec{q}_r) \tag{4}$$

Dimensionless variables are defined using the following scaling:

$L = L'/4\sigma T_0^4,\ P = P'/\rho V_0^2,\ Q_r = q_r/4\sigma T_0^4,\ T = (T' - T_0)/\Delta T\ ,\ t = t' V_0/H\ ,\ V_0 = (\mu/\rho H)\sqrt{Ra},$
$U = u/V_0\ ,V = v/V_0\ ,X = x/H, Y = y/H\ ,\theta_0 = T_0/(T_H - T_C), T_0 = (T_H + T_C)/2$

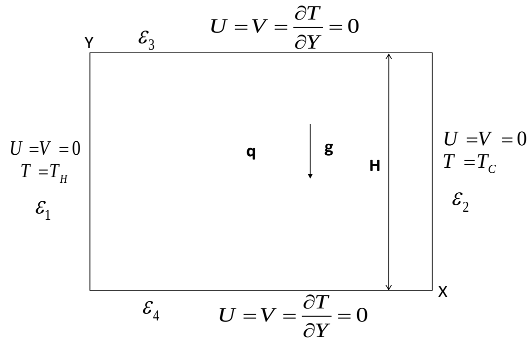

Figure 1. Physical geometry and boundary conditions

Accordingly, the dimensionless governing equations are expressed for an unsteady bi-dimensional problem:

$$\frac{\partial U}{\partial X} + \frac{\partial V}{\partial Y} = 0 \tag{5}$$

$$\frac{\partial U}{\partial t} + U\frac{\partial U}{\partial X} + V\frac{\partial U}{\partial Y} = \frac{-\partial P}{\partial X} + \frac{1}{\sqrt{Ra_E}}\left(\frac{\partial^2 U}{\partial X^2} + \frac{\partial^2 U}{\partial Y^2}\right) \tag{6}$$

$$\frac{\partial V}{\partial t} + U\frac{\partial V}{\partial X} + V\frac{\partial V}{\partial Y} = \frac{-\partial P}{\partial Y} + \frac{1}{\sqrt{Ra_E}}\left(\frac{\partial^2 V}{\partial X^2} + \frac{\partial^2 V}{\partial Y^2}\right) + \frac{1}{Pr}T \tag{7}$$

$$\frac{\partial T}{\partial t} + U\frac{\partial T}{\partial X} + V\frac{\partial T}{\partial Y} = \frac{1}{Pr\sqrt{Ra_E}}\left(\frac{\partial^2 T}{\partial X^2} + \frac{\partial^2 T}{\partial Y^2}\right) + \frac{Ra_I}{Pr Ra_E^{\frac{3}{2}}} - \frac{1}{Pr\sqrt{Ra_E}}\frac{\theta_0}{Pl}div(\vec{Q}_r) \tag{8}$$

The term $\mathrm{div}(Q_r)$ in the energy equation representing radiative exchange rate in the cavity is determined from the solution of the radiative transfer equation, which can be put in the following form for an absorbing, emitting, and scattering medium:

$$\mu\left(\frac{\partial L}{\partial X}\right)+\eta\left(\frac{\partial L}{\partial Y}\right)+\tau L=\frac{\tau}{4\pi}\left[(1-\omega)\left(1+\frac{T}{\theta_0}\right)^4+\omega\int_{4\pi}\mathrm{L}d\Omega\right] \quad (9)$$

$$div(Q_r)=\tau(1-\omega)\left[\left(1+\frac{T}{\theta_0}\right)^4-\int_{4\pi}Ld\Omega\right] \quad (10)$$

$\mathrm{L}(\mathrm{X},\mathrm{Y},\vec{\Omega})$ is the dimensionless radiation intensity at position (X, Y) in the direction $\vec{\Omega}=\mu\vec{\imath}+\eta\vec{\jmath}$
The boundary conditions for reflecting and emitting isothermal opaque walls are as follows:

$U=V=0\ ,T=T_H$ at $X=0,Y\in[0,1]$

$U=V=0\ ,T=T_C$ at $X=1\ \ ,Y\in[0,1]$

$\mathrm{U}=\mathrm{V}=0,\frac{\partial \mathrm{T}}{\partial \mathrm{Y}}=0$ at $Y=0\ ,X\in[0,1]$

$U=V=0,\ \frac{\partial T}{\partial Y}=0$ at $Y=1,X\in[0,1]$

The radiative boundary conditions are:

- for vertical walls ($\varepsilon_1=\varepsilon_2=1$):

$L(0,Y)=\frac{1}{4\pi}\left(1+\frac{T(0,Y)}{\theta_0}\right)^4 atX=0\ ,\mu<0$

$L(1,Y)=\frac{1}{4\pi}\left(1+\frac{T(1,Y)}{\theta_0}\right)^4 atX=1\ ,\mu>0$

- for horizontal walls ($\varepsilon_3=\varepsilon_4=0$):
$L(X,0)=\frac{1}{\pi}Q_{inc}(X,0)$ at $Y=0\ ,\eta<0$

$L(X,1)=\frac{1}{\pi}Q_{inc}(X,1)$ at $Y=1,\eta>0$

Q_{inc} is the incident radiation flux obtained by:

$$Q_{inc}(X,0)=\sum_{\eta_m<0}|\eta_m|\omega_m L(X,0) \text{ at } Y=0 \quad (11)$$

$$Q_{inc}(X,1)=\sum_{\eta_m>0}|\eta_m|\omega_m L(X,1) \text{ at } Y=1 \quad (12)$$

3. Numerical modeling

The solutions of radiative transfer equation (RTE) are obtained by the discrete ordinates method [31, 32], and the angular space is discretized by the S6 quadrature. The 2D governing equations are solved numerically by a finite-volumes scheme using the staggered arrangement. Eqs. (5)-(8) were discretized in time by a second-order backward Euler scheme in which the diffusive and viscous linear terms are implicitly treated while the convective nonlinear terms are explicitly treated using an Adamse-Bashforth extrapolation. The spatial discretization applied is based on a non-uniform grid refined in the vicinity of the vertical walls by using Chebychev collocation points. A technique derived from the classical projection method is employed to solve the coupling between pressure and velocity.

The Poisson equations for the pressure correction in the projection method are solved by standard multigrid techniques [25].

4. Heat transfer parameters

The non-dimensional heat transfer rate in terms of local convective and radiative Nusselt numbers, Nu_{cv} and Nu_R, are given by [30] :

$$Nu_{cv}(Y) = -\left(\frac{\partial T}{\partial X}\right)_{X=0,1} \tag{13}$$

$$Nu_R(Y) = \frac{\theta_0}{Pl}\left[Q_R^{net}\right]_{X=0,1} \tag{14}$$

Where $Q_R^{net}|_{X=0,1}$ is the dimensionless net radiative flux density at the hot or cold vertical walls defined by [30]:

$$Q_R^{net}(Y)|_{X=0,1} = \varepsilon_p\left[\frac{1}{4}\left(1+\frac{T}{\theta_0}\right)^4 - \sum|\mu_m|\omega_m L(X,Y)\right]_{X=0,1} \tag{15}$$

The total average Nusselt number is calculated by summing the average convective Nusselt number and the average radiative Nusselt number [30]:

$$\overline{Nu}_T = \overline{Nu}_{cv} + \overline{Nu}_R = \int_0^1 -\left(\frac{\partial T}{\partial X}\right)_{X=0,1} dY + \frac{\theta_0}{Pl}\int_0^1 \left[Q_R^{net}\right]_{X=0,1} dY \tag{16}$$

5. Grid sensitivity and validation

The mesh sensitivity test was performed for six uniform meshes comparing the average total and radiative Nusselt numbers on the hot wall in steady state. The studied configuration is characterized by the following calculation parameters: $Ra_I = 4\times10^4$, $Ra_E = 10^6$, $\tau = 1$, $Pl = 0.02$ and $\theta_0 = 1.5$. The medium is initially at rest and at a uniform temperature $T_0 = 300\text{K}$, for which $Pr = 0.71$. Table 1 shows the results obtained in a domain where the meshes vary from (33×33) to (257×257). We notice that as the mesh gets finer, the values of the average radiative and total Nusselt decrease. For the meshes (161×161) and (257×257), the results give almost similar values which testifies that the solution becomes independent of the mesh beyond (161×161). The latter is considered the best compromise between accuracy and computation time and is used to validate our code.

Table 1. Grid size effect on the average total and radiative Nusselt numbers

Mesh	33x33	57x57	97x97	129x129	161x161	257x257
$\overline{Nu}_T$	17.32	17.32	16.98	16.96	16.21	16.21
$\overline{Nu}_R$	10.566	10.563	10.481	10.470	10.44	10.44

In order to check on the accuracy of the numerical techniques employed for the solution of the problem considered in this study, we performed two test cases given in the literature. First, we validated our radiation code to verify the accuracy of the discrete ordinate method. The simulations were performed on a square cavity containing a gray participating medium in radiative equilibrium. The walls are assumed to be black and they are held at zero intensity (cold walls) except for the top surface which has unit intensity (hot wall). The curves in fig. 2 compare the predictions of the flux on the hot wall, given by quadratures S4 and S6, with the exact solution of Crosbie and Schrenker [33] for an optical thickness τ=0.25. Both quadratures give accurate predictions, but it can be noted that the S6 quadrature is slightly more accurate than S4. A mean deviation of 0.4% was observed for the S6 quadratures compared to 0.5% for the S4 quadratures. It is also interesting to note that El Kasmi [34] showed in his study that the three quadratures S4, S6 and S8 give accurate predictions and that if we use a mesh larger than 40 x40 elements, the S4 quadrature loses accuracy and the S6 quadrature is the most accurate.

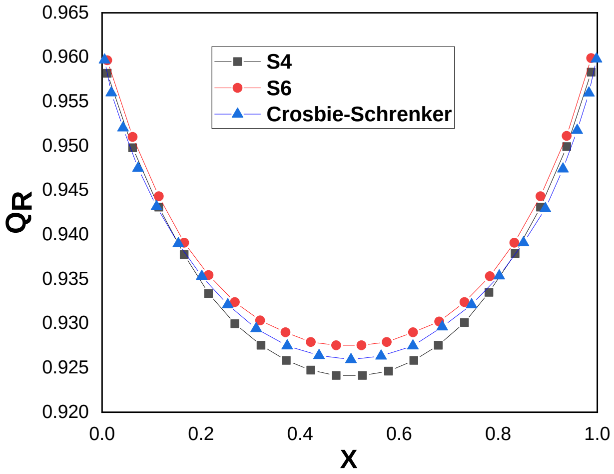

Figure 2. Dimensionless radiative flux on the hot wall for quadratures S_4 and S_6. τ=0.25 and ω=0

The second test case consists in verifying the natural convection code by comparing our results with those available in the literature, in the case of internal heat generation, for $Pr = 0.71$, $Ra_E = 10^5$ and $Ra_I = 10^5, 10^7$. Average Nusselt along the hot wall and extreme values of the stream function ψ_{max} and ψ_{min} are compared with those given by Shim and Hyun [35] and Oztop et al. [36], as shown in table 2. Outcomes of the present work are within those given in the literature. A good agreement was found between the present calculations and those reported in the work of Oztop et al. [36] with a maximum deviation of 2.9% obtained for ψ_{max} at $Ra_I=10^6$ and 2.3% for $\overline{Nu}$ at $Ra_I=10^7$. Compared to the results of Shim and Hyun [35], except for the average Nusselt number which shows quite large differences with respect to our results and those of Oztop et al. [36], low differences are also noted for ψ_{max} and ψ_{min}, 1.86% and 1.12% for $Ra_I=10^6$ and 0.006% and 2.8% for $Ra_I=10^7$.

Table 2. Comparison of the average Nusselt number with other studies for $Pr = 0.71$ and $Ra_E = 10^5$

Ra_I	Shim and Hyun [35]			Present results			Oztop et al. [36]		
	ψ_{max}	ψ_{min}	$\overline{Nu}$	ψ_{max}	ψ_{min}	$\overline{Nu}$	ψ_{max}	ψ_{min}	$\overline{Nu}$
10^6	1.56	-17	-0.01	1.531	-16.81	0.096	1.488	-16.720	0.098
10^7	16.4	-24.5	-66	16.401	-23.813	-43	16.286	-23.711	-44

6. Results and discussions

The fixed parameters of simulation are $Pl = 0.02$ and $Ra_E = 10^6$. However, we consider different values of internal Rayleigh number varying from 0 to 4×10^{12}. The effects of external heating and internal heat generation on the natural convection of a transparent and semi-transparent fluid in a differentially heated cavity can be seen in figs. 3-9. In the presence of internal heating, the fields of flow and temperature take a different structure from the case where $Ra_I = 0$.

For a low internal Rayleigh number($Ra_I \leq 4 \times 10^4$), the results show that there is no effect of internal heat generation. Isotherms and streamlines are almost similar (figs. 3 and 4 for case $\omega = 0.25$ and 0). Analysis of the figures shows that internal production is relatively low. The flow is assigned to the presence of one cell circulating clockwise; it occupies a large part of the cavity, and secondary and tertiary eddies appear inside the cavity for $\omega = 0.5$ and $\omega = 0.75$. In the absence of internal heat generation, isotherms and streamlines are little affected by the diffusion coefficient with a slight acceleration of the flow field in the cavity. When ω reache 1, pure natural convection profiles are found. Moreover, the radiation effect decreases with increasing ω value and the isotherms are similar to those of the pure natural convection (CP). It is deduced from the comparison between the non-scattering case and the case of the absorbing-scattering medium that there is less radiation absorbed in the latter case. Thus, the temperature distribution is the same in the case of a non-diffusing fluid (figs. 3 and 4) but affected by variations in Albedo. For a participating medium ($\omega > 0$), we notice that cavity nucleus is more heated in comparison with pure convection case (CP), which indicated a strong deformation of the temperature gradient near the cold wall. We note that the effect of the internal generation in the cavity ($Ra_I = 4 \times 10^4$) is more remarkable when the albedo coefficient becomes important (ω=0.5 and ω=0.75).

When the heat production increases ($Ra_I > 4 \times 10^4$), the overall thermal energy in the cavity increases too. Its small vortices are merged to the primary vortices with relatively higher circulation intensity than the lower value of Ra_I . Thus, a small counter-clockwise cell appears on the left side and moves to the left with increasing Ra_I. The resistance in this new cell increases also as the internal heat production increases in amplitude. For a large internal Rayleigh number, the whole cavity is occupied by two recirculating counter-clockwise and clockwise cells near the hot and cold walls respectively, due to the negative and positive buoyancy effect respectively. The sinking motion near the cold wall is intensified compared to that near the hot wall due to the differential buoyancy effect. With increasing Ra_I, the circulations take on an irregular shape due to the vigorous sinking motion caused by the higher interior temperatures. Thereby, the presence of the internal heat generation causes an enhancement of heat exchange leading to an increase in the average total Nusselt number up to 609.2 for ω=0 and $Ra_I = 4 \times 10^{12}$ (table 3). Isotherms have a tendency to be horizontally uniform and vertically linear in the upper part of the surrounding wall ($Ra_I = 4 \times 10^{12}$). However, in the lower part of the cavity, isotherms are divided in two groups. The maximal temperature between the hot and cold surfaces can exceed 42, which explains why the fluid rises in the central regions of the surrounding wall and falls along the hot and cold walls. The relative strengths of the recirculation flow are related to the thermal gradients, which are weaker near the hot wall than near the cold wall. Along the vertical walls, the isotherms become tighter and the thermal boundary layers get thinner as the effect of internal heat generation increases.

In the presence of relatively low internal heat generation, the non-linearity of the radiation with temperature breaks the central symmetry and the flow becomes unicellular occupying the entire cavity. The total thermal energy in the cavity is on increase. It should be noted that the thermal boundary layer behavior at the hot and cold walls is affected as the albedo increases. Generally, temperatures levels for a radiative fluid are lower and more uniform than for a non-radiative fluid because radiation gives a supplementary mechanism for transferring the generated heat inside the cavity. Thus, the flow near the heated wall decays and weakens considerably. The characteristic counterclockwise flow prevails on the active cavity walls.

The variation of global, radiative and convective average Nusselt numbers as a function of Albedo and Ra_I is presented in table 3. A general view of the results show that the global and radiative Nusselt numbers decrease with increasing Albedo and increase with Ra_I increasing. The minimum values of $\overline{Nu}_R$ and $\overline{Nu}_T$ are obtained at ω=0.75 and Ra_I=0, and are respectively equal to 2.83 and 6.203. We can see that for low heat generation, the convective Nusselt number has positive values, and from $Ra_I=4\times10^{11}$ the values are negative. This means that, due to the internal heat generation, heat is transferred from the fluid to the hot wall. The latter absorbs the heat from the fluid at internal temperature. Generally, for diffusing environments, Albedo effect on flow field is limited to a slight acceleration of the velocity field of the cavity nucleus. Since the order of magnitude of the external heating is comparable to the internal heat generation, the positive value of the global average Nusselt number indicates that there is upward movement near the hot wall although the circulation experiences a slowdown due to the buoyancy effect generated by the internal heat generation. Therefore, as Ra_I increases, the average convective Nusselt number ($\overline{\mathrm{Nu}}_{\mathrm{cv}}$) decreases. It increases in the negative direction indicating a downward motion near the hot sidewall, which means that the hot wall absorbs heat from the higher temperature interior fluid. Comparing the case of a non-scattering fluid ($\omega = 0$) with an absorbing-scattering fluid ($\omega \neq 0$), it appears that the latter case has the least absorption of radiation. That is, the temperature distribution is somewhat similar to that of an optically thinner non-scattering fluid. However, when the effect of internal heat generation is taken into account, the core of the cavity is found to be more heated than the case (Ra_I = 0). It is interesting to note that the effect of the internal heat generation is more visible for ω = 0. We can observe the effect of the contribution of the internal source term on flows. When the medium is participating, the internal source effect is important.

Table 3. Variation of average convective, radiative and total Nusselt numbers on the hot wall as a function of ω and Ra_I

Ra_I	CP	$\omega = 0$			$\omega = 0.25$			$\omega = 0.5$			$\omega = 0.75$		
	$\overline{Nu}_{cv}$	$\overline{Nu}_{cv}$	$\overline{Nu}_R$	$\overline{Nu}_T$	$\overline{Nu}_{cv}$	$\overline{Nu}_R$	$\overline{Nu}_T$	$\overline{Nu}_{cv}$	$\overline{Nu}_R$	$\overline{Nu}_T$	$\overline{Nu}_{cv}$	$\overline{Nu}_R$	$\overline{Nu}_T$
0	8.875	5.775	10.44	16.21	4.534	7.924	12.46	3.264	4.515	7.779	3.374	2.830	6.203
4×10^4	8.875	5.775	10.44	16.21	10.22	29.61	39.84	15.67	51.80	67.47	18.70	68.19	86.89
4×10^{11}	-131.8	-20.14	77.82	57.68	-14.22	34.43	20.21	-13.10	138.9	125.8	-198.3	259.0	60.7
4×10^{12}	-1399	-195.9	805.1	609.2	-182.2	639.5	457.3	-183.5	517.5	334	-225.6	412.8	187.2

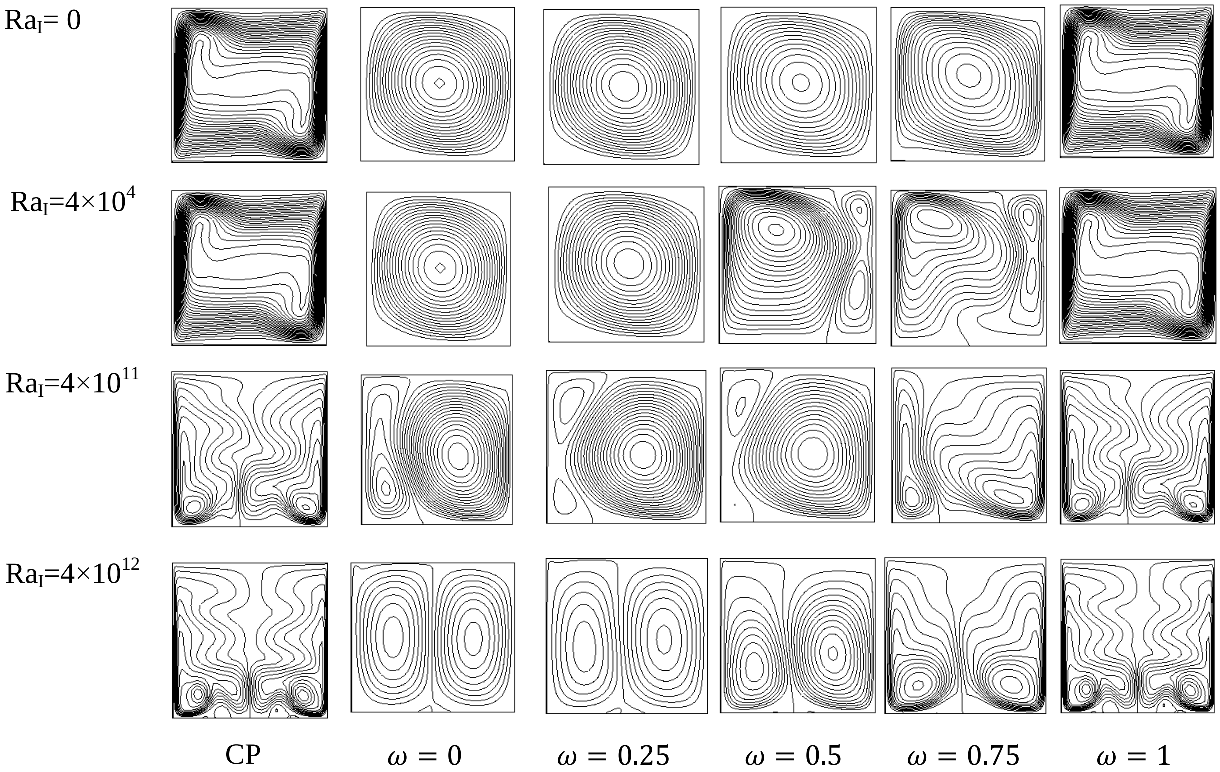

Figure 3. Streamlines as a function of Ra_I and ω for $\tau = 1$

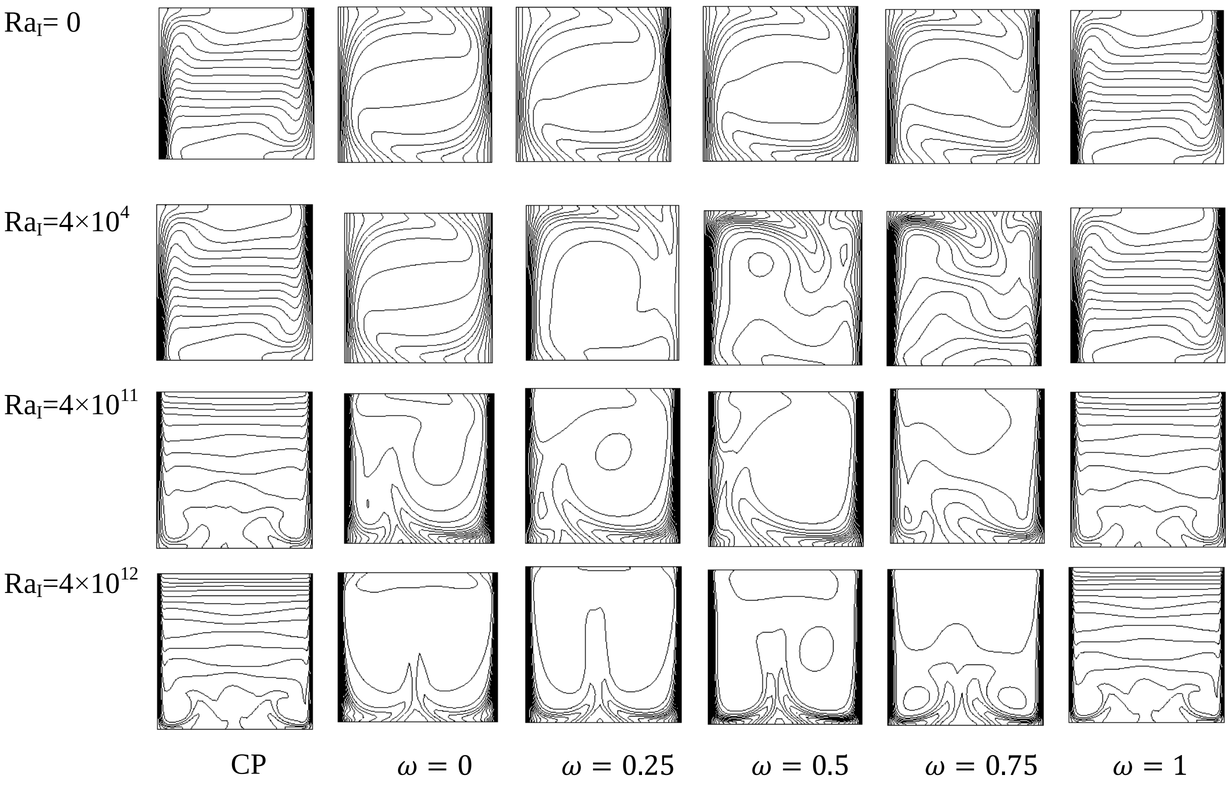

Figure 4. Isotherms as a function of Ra_I and ω for $\tau = 1$

The analysis of figs. 6, 7 and 8 shows that the influence of the optical thickness τ on the maximal velocity (vertical and horizontal) is relatively important. One can notice that there is an increase in these velocities as a function of τ. The vertical velocity peaks are significantly affected by the Albedo coefficient ω. For τ=10, they decrease from 4.4 for ω = 0 to 1.26 for ω = 0.5. The boundary layers move closer to the active walls and their thickness increases with increasing τ. The temperature profiles at the median line for different values of τ are shown on figs. 5 and 8. Analysis of these figures shows that the temperatures on the horizontal mid-plane decrease with increasing optical thickness. Indeed, on the vertical median (X=0.5) and for ω =0.5, the temperature goes from 43.3 for τ = 0 to 2.35 for τ=5.

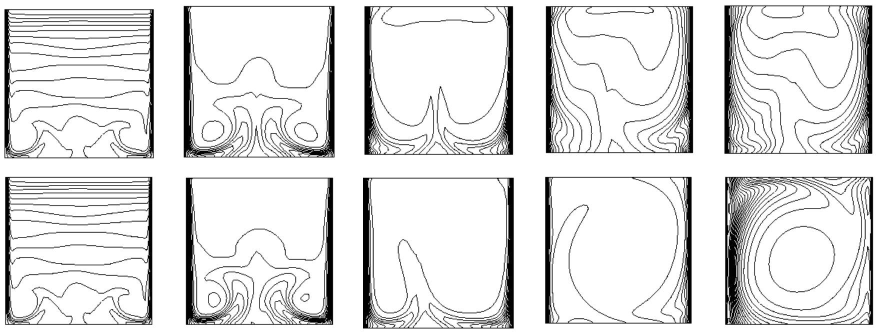

$\tau = 0$ $\tau = 0.2$ $\tau = 1$ $\tau = 5$ $\tau = 10$

Figure 5. Isotherms for ω = 0 (top), ω = 0.5 (bottom) and $Ra_I = 4 \times 10^{12}$

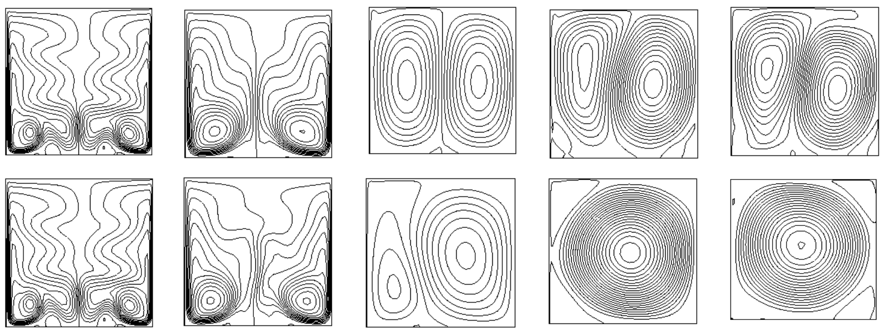

$\tau = 0$ $\tau = 0.2$ $\tau = 1$ $\tau = 5$ $\tau = 10$

Figure 6. Streamlines for ω = 0 (top), ω = 0.5 (bottom) and $Ra_I = 4 \times 10^{12}$

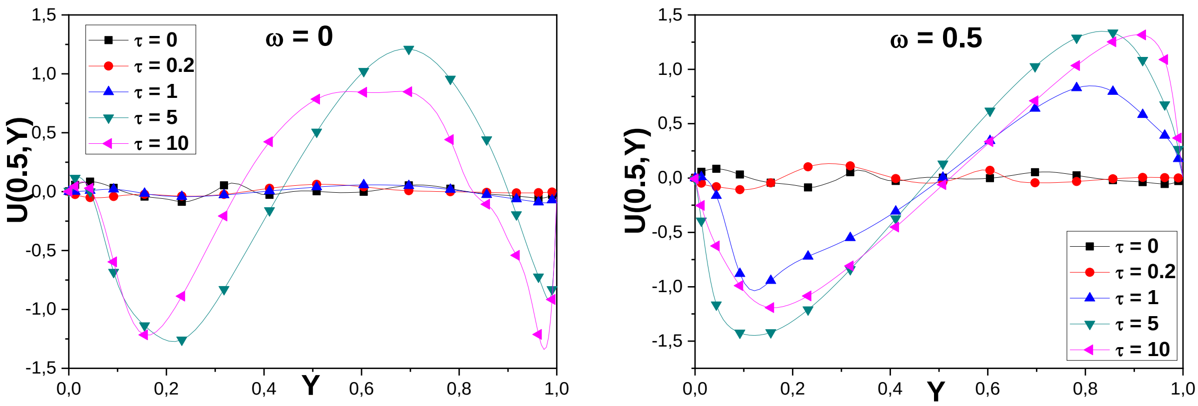

Figure 7. Horizontal velocity at the vertical cross-section according to τ for $Ra_I = 4 \times 10^{12}$

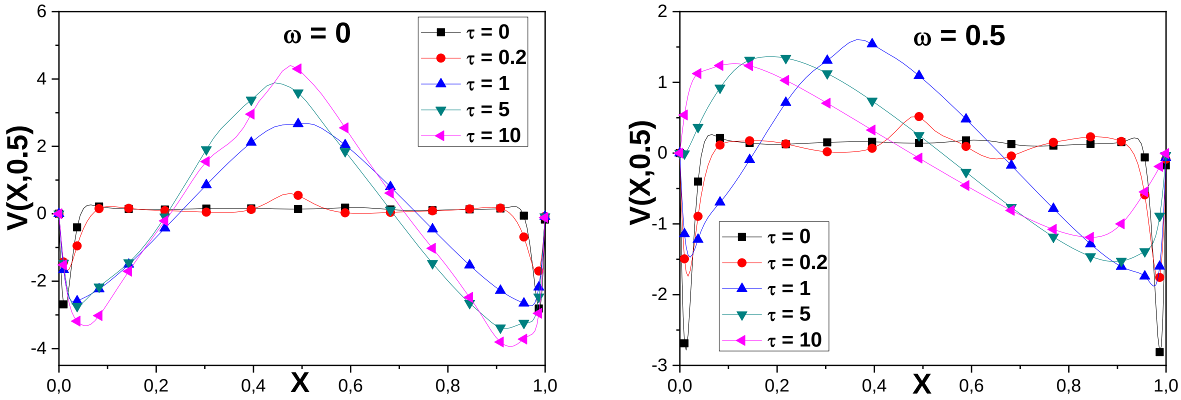

Figure 8. Vertical velocity at the horizontal cross-section according to τ for $Ra_I = 4 \times 10^{12}$

The variations of the total and radiative Nusselt numbers as a function of the optical thickness for $\mathrm{Ra_I} = 4 \times 10^{12}$ are shown in table 4. Regarding the variation of the average Nusselt numbers, we observe, in general, that increasing the optical thickness leads to a decrease in the average Nusselt numbers. Similarly, in the case of an absorbing-diffusing fluid, the increase of the optical thickness leads to a decrease of the heat exchanges within the cavity. This indicates that radiation affects flow even in the presence of internal heat generation.

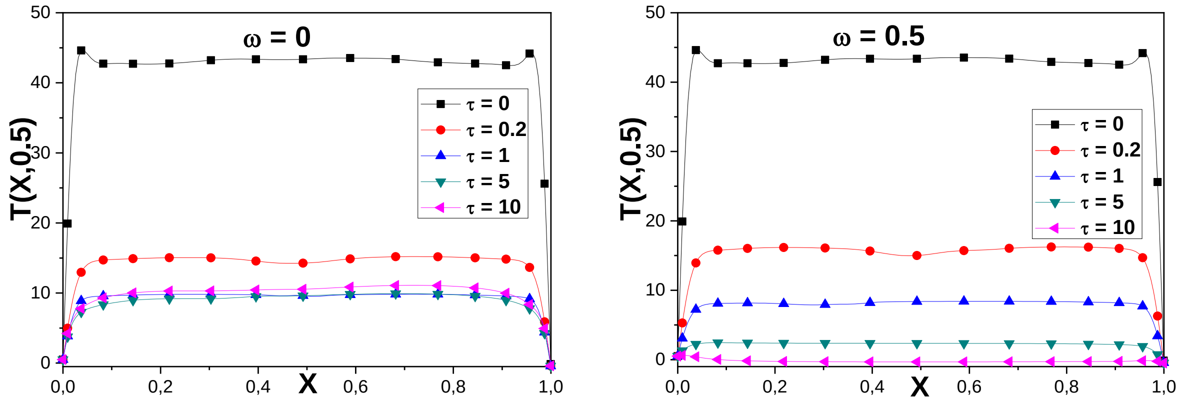

Figure 9. Temperature profiles at mid-height according to τ for $Ra_I = 4 \times 10^{12}$

Table 4. Variation of average convective, radiative and total Nusselt numbers on the hot wall as a function of optical thickness τ and ω for $Ra_I = 4 \times 10^{12}$

τ	$\omega = 0$			$\omega = 0.5$		
	$\overline{Nu}_{cv}$	$\overline{Nu}_R$	$\overline{Nu}_T$	$\overline{Nu}_{cv}$	$\overline{Nu}_R$	$\overline{Nu}_T$
0	-1399	7.736	1406	-1399	7.736	1406
0.2	-266	749.8	1016	-282.3	444.3	726.6
1	-195.9	805.1	1001	-149.2	336.2	485.4
5	-227.1	778.9	1006	-55.74	47.62	103.4
10	-273.5	742.1	1016	-13.63	27.70	41.33

7. Conclusion

Coupled natural convection and volumetric radiation in presence of internal heat generation source is studied numerically in a differentially heated square cavity. The two dimensional flow is described by the Navier–Stokes equations coupled with energy equation and radiative transfer equation. The present study shows the effects of the internal Rayleigh number, albedo coefficient, and optical thickness on the flow and heat transfer. In view of the results presented, the main points can be summarized as follows:

- internal heat generation significantly alters flow and temperature fields;
- increase in the value of the heat generation parameter translates into an increase in the flow rates in the secondary cell as well as an increase in its size until it occupies half of the total space of the cavity. A further increase in the heat generation value causes the development of more cells and an increase in the temperature of the fluid in the cavity;
- as the effect of internal heat generation increases, the isotherms appear to be tighter and the thermal boundary layers get thinner along the active walls;
- presence of the internal heat generation causes an enhancement of heat exchange leading to an increase in the average total Nusselt number;
- increase in optical thickness leads to a decrease in temperature and heat exchange within the cavity

Acknowledgments

Authors gratefully acknowledge the financial support of the Directorate General for Scientific Research and Technological Development (DGRSDT).

Nomenclature

C_p– specific heat capacity, [J kg $^{-1}$ K^{-1}]
g– gravitational acceleration , [m s^{-2}]
H–dimension of the enclosure, [m]
k– thermal conductivity, [W m^{-1} K^{-1}]
L – dimensionless radiation intensity, [-]
Nu– Nusselt number, [-]
Pl– Planck number $(= k/4H\sigma T_0^3)$, [-]
Pr– Prandtl number $(= \nu/\alpha)$, [-]
P– dimensionless pressure, [-]
Q_{inc} – dimensionless incident radiative flux, [-]
q – internal heat generation, [W m^{-3}]
Q_r –dimensionless radiative heat flux, [-]
q_r –radiative heat flux [W m^{-2}]
Ra_E– external Rayleigh number $(= \frac{g\beta\Delta T H^3}{\nu\alpha})$, [-]
Ra_I– internal Rayleigh number $(= \frac{g\beta q H^5}{\nu\alpha k})$, [-]
T– dimensionless temperature, [-]
t– dimensionless time, [-]
U, V–dimensionless velocity-components, [-]
u, v–dimensional velocity-components, [m.s^{-1}]
X, Y – dimensionless co-ordinates, [-]
x, y – Cartesian coordinates, [m]

Greek symbols

α– thermal diffusivity, $(= k/\rho Cp)$, [m^{2}s^{-1}]
β– thermal expansion coefficient, [K^{-1}]
ε– Emissivity, [-]
κ – absorption coefficient, [m^{-1}]
ν– kinematic viscosity, [m^2 s^{-1}]
ρ– fluid density, [kg m^{-3}]
σ– Stefan-Boltzmann constant, [w m^{-2} K^{-4}]
μ, η– direction cosines
ω– albedo coefficient , [-]
ω_m– weight in the direction Ω_m
τ– optical thickness $(= Hk_a)$, [-]
θ_0– dimensionless reference temperature $(= \frac{T_0}{T_H - T_C})$, [-]

Subscripts

‘ – dimensional variables
0 –reference state
cv– convective
C– Cold
H – Hot
R– Radiative
T – Total

References

[1] Mckenzie, D. P., *et al.*, Convection in the Earth's Mantle: Toward a Numerical Simulation, *J. Fluid Mech.*, 62 (1974), 3, pp. 465-538

[2] Travis, B., *et al.*, Three-Dimensional Convection Planforms with Internal Heat Generation, *Geophys. Res. Lett.*, 17(1990), pp. 243-246

[3] Sharma, A. K., *et al.*, Conjugate Transient Natural Convection in a Cylindrical Enclosure with Internal Volumetric Heat Generation, *Ann. Nucl. Energy,* 35(2008), 8, pp. 1502-1514

[4] Lee, S. D., *et al.*, Natural Convection Thermo Fluid Dynamics In a Volumetrically Heated Rectangular Pool, *Nucl. Eng. Des.*, 237(2007), 5, pp. 473-483

[5] G. Lauriat, Combined Radiation-Convection in Gray Fluids Enclosed in Vertical Cavities, *J. Heat Transfer,* 104(1982), 4, pp. 609-615

[6] Yücel, A., *et al.*, Natural Convection and Radiation in a Square Enclosure, *Numer. Heat Tr. A-Appl.*, 15 (1989), 2, pp. 261-278

[7] Draoui, A., *et al.*, Numerical Analysis of Heat Transfer by Natural Convection and Radiation in Participating Fluids Enclosed in Square Cavities, *Numer. Heat Tr. A-Appl.*, 20 (1991), 2, pp. 253-261

[8] Fusegi, T., Farouk, B., Laminar and Turbulent Natural Convection-Radiation Interactions in a Square Enclosure Filled with a Nongray Gas, *Numer. Heat Tr. A-Appl.,* 15(1989), 3, pp. 303-322

[9] Tan, Z., Howell, J. R., Combined Radiation and Convection in a Two-Dimensional Participating Square Medium, *Int. J. Heat Mass Transfer,* 34(1991), 3, pp. 785-793

[10] G Colomer, G., *et al.*, Three-Dimensional Numerical Simulation of Convection and Radiation in a Differentially Heated Cavity Using the Discrete Ordinates Method, *Int. J. Heat Mass Transfer*, 47 (2004), 2, pp. 257-269

[11] Ibrahim, A., Coupling of Natural Convection and Radiation in Absorbing-Emitting Gas Mixtures (in French language), Ph. D. thesis, University of Poitiers, France, 2010

[12] Laouar-Meftah, S., *et al.*, Comparative Study of Radiative Effects on Double Diffusive Convection in Non gray Air-CO_2 Mixtures in Cooperating and Opposing Flow, *Math. Probl. Eng.*, (2015), pp. 1-17

[13] Moufekkir, F., *et. al.*, Numerical Prediction of Heat Transfer by Natural Convection and Radiation in an Enclosure Filled with an Isotropic Scattering Medium, *J. Quant. Spectrosc. Radiat. Transf.*, 113 (2012), 13, pp. 1689-1704

[14] Lari, K., *et al.*, Combined Heat Transfer of Radiation and Natural Convection in a Square Cavity Containing Participating Gases, *Int. J. Heat Mass Transfer*, 54(2011), 23-24, pp. 5087-5099

[15] Liu, X., *et al.*, Combined Natural Convection and Radiation Heat Transfer of Various Absorbing-Emitting-Scattering Media in a Square Cavity, *Adv. Mech. Eng.*, 6(2015), pp. 403690-1-10

[16] Mezrhab, A., *et al.*, Numerical Study of Double-Diffusion Convection Coupled to Radiation in a Square Cavity Filled with a Participating Grey Gas, *J. Phys. D: Appl. Phys.*, 41(20), 19, pp. 195501-1-16

[17] Byun, K.-H., HyukIm, M., Radiation Laminar Free Convection in a Square Duct with Specular by Absorbing-Emitting Medium, *KSMEI Int. J.*, 16(2002), 10, pp. 1346-1354

[18] Kumar, P., Eswaran, V., A Numerical Simulation of Combined Radiation and Natural Convection in a Differential Heated Cubic Cavity, *J. Heat Transfer*, 132(2010), pp. -1-13

[19] Chaabane, R., *et. al.*, Numerical Study of Transient Convection with Volumetric Radiation Using an Hybrid Lattice Boltzmann BGK-Control Volume Finite Element Method, *J. Heat Transfer*, 139(2017), 9, pp.1-7

[20] Balaji, C. Venkateshan, S. P., Interaction of Surface Radiation with Free Convection in a Square Cavity, *Int. J. Heat Fluid Flow,* 14(1993), 3, pp. 260–267

[21] Akiyama, M., Chong, Q. P., Numerical Analysis Of Natural Convection with Surface Radiation in a Square Enclosure, *Numer. Heat Tr. A-Appl.*, 32(1997), pp. 419-433

[22] Lauriat, G., Desrayaud, G., Effect of Surface Radiation on Conjugate Natural Convection in Partially Open Enclosures, *Int. J. Therm. Sci.*, 45 (2006), 4, pp. 335-346

[23] Wang, H., et.*al.*, Numerical Study of Natural Convection-Surface Radiation Coupling in Air-Filled Square Cavities, *C.R. Mec.*, 334 (2006), 1, pp. 48-57

[24] Hamimid, S., *et al.*, Numerical Simulation of Combined Natural Convection Surface Radiation for Large Temperature Gradients, *J. Thermophys. Heat Transfer*, 29 (2015), 3, pp.1509-1517

[25] Bouafia, M., *et al.*, Non-Boussinesq Convection in a Square Cavity with Surface Thermal Radiation, *Int. J. Therm. Sci.*, 96 (2015), pp.236-247

[26] Ashraf, M., *et al.*, Computational Analysis of the Effect of Nano Particle Material Motion on Mixed Convection Flow in the Presence of Heat Generation and Absorption, *CMC-Comput. Mater. Con.*, 65 (2020), 2, pp. 1809-1823

[27] Waqas, M., *et al.*, Interaction of Heat Generation in Nonlinear Mixed/Forced Convective Flow of Williamson Fluid Flow Subject to Generalized Fourier's and Fick's Concept, *J. Mater. Res. Technol.*, 9 (2020), 5, pp. 11080-11086

[28] Elbashbeshy, E. M. A., et al., Effect of Thermal Radiation on Free Convection Flow and Heat Transfer over a Truncated Cone in the Presence of Pressure Work and Heat Generation/Absorption, *Thermal Science*, 20 (2016), 2, pp. 555-565

[29] Hamimid, S., *et al.*, Numerical Analysis of Combined Natural Convection-Internal Generation Source-Surface Radiation, *Thermal Science*, 20 (2016), 6, pp. 1879-1889.

[30] Rachedi, N., *et al.*, Effect of Radiation on the Flow Structure and Heat Transfer in a 2-D Gray Medium, *Thermal Science*, 23(2019), 6A, pp. 3603-3614

[31] Modest, M. F., *Radiative Heat Transfer*, 2nd ed., Academic Press, Sandi ego, USA, 2003

[32] Fiveland, W. A., Discrete-Ordinates Solutions of the Radiative Transport Equation for Rectangular Enclosures, *J. Heat Transfer*, 106(1984), 4, pp. 699-706

[33] Crosbie, A. L., Schrenker, R. G., Exact Expression for Radiative Transfer in a Three-Dimensional Rectangular Geometry, *J. Quant. Spectrosc. Radiat. Transf.*, 28 (1982), 6, pp. 507-526

[34] El Kasmi, A., Application Of The Discrete Ordinate Method to Radiative Transfer in Complex Two-Dimensional Geometries, Radiation-Convection Coupling (in French language), Master's thesis, University of Quebec, Canada, 1999

[35] Shim, Y.M., *et al.*, Transient Confined Natural Convection with Internal Heat Generation, *Int. J. Heat Fluid Flow*, 18(1997), pp. 328-333

[36] Oztop, H. F., *et al.*, Natural Convection in Wavy Enclosures with Volumetric Heat Sources, *Int. J. Therm. Sci.*, 50(2011), pp. 502-514

Received: 06.06.2022.
Revised: 01.09.2022.
Accepted: 08.09.2022.